Bioorganic & Medicinal Chemistry Letters 24 (2014) 2057–2061

Contents lists available at ScienceDirect

Bioorganic & Medicinal Chemistry Letters

journal homepage: www.elsevier.com/locate/bmcl

Discovery and SAR of a novel series of 2,4,5,6-tetrahydrocyclopenta[*c*]pyrazoles as N-type calcium channel inhibitors

Michael P. Winters *, Nalin Subasinghe, Mark Wall, Edward Beck, Michael R. Brandt, Michael F. A. Finley, Yi Liu, Mary Lou Lubin, Michael P. Neeper, Ning Qin, Christopher M. Flores, Zhihua Sui

Janssen Research and Development, LLC, 1400 McKean Rd., Spring House, PA 19477, USA

ARTICLE INFO

Article history:
Available online 28 March 2014

Keywords:
2,4,5,6-Tetrahydrocyclopenta[*c*]pyrazoles
N-type calcium channel
$Ca_v2.2$ blockers
Pain
Rat CFA model

ABSTRACT

A novel series of substituted 2,4,5,6-tetrahydrocyclopenta[*c*]pyrazoles were investigated as N-type calcium channel blockers ($Ca_v2.2$ channels), a chronic pain target. One compound was active in vivo in the rat CFA pain model.

N-type calcium channels ($Ca_v2.2$ channels) have been implicated in the neurotransmission of pain.[1] They are highly expressed in the dorsal horn of the spinal cord and are frequently up-regulated in pain syndromes.[2] In addition, N-type knockout mice have reduced nociceptive sensitivity.[3] There is also a marketed drug, the cone snail toxin ziconotide (Prialt®), that is a potent blocker of N-type calcium channels. Ziconotide is prescribed for severe chronic pain and is limited to intrathecal administration.[4] In addition, it has a side-effect profile that gives it a very narrow therapeutic window.[4] Due to these limitations, many groups have tried to develop novel oral N-type calcium channel inhibitors for the treatment of chronic pain.[5]

One hit from a screen of our compound collection was pyrazole **1**, a 100 nM inhibitor of the N-type calcium channel (Fig. 1). It was hypothesized that rigidifying the sidechain of **1** by forming a fused cyclopentane ring on the pyrazole scaffold might improve potency by lessening the rotational degrees of freedom of the sidechain. This novel ring system also gives a favorable IP position. Pharmacophore modeling of the 2 scaffolds showed that the 2,3,5-substitued tetrahydrocyclopenta[*c*]pyrazole **2** filled very similar space to **1** and should be a good substitute for the straight chain scaffold. Compound **3** was one of a few compounds initially made to assess the activity and selectivity of the series and was found to be 26 nM for N-type in the Functional Drug Screening System (FDSS) assay but only have 17 and 62% inhibition of L-type calcium channel at 1 and 5 μM, respectively.[6,7] Rat liver microsome (RLM) and human liver microsome stability (HLM) of **3** was low, and metabolic ID in both species indicated that loss of the methyl from the 2-methoxy was the major metabolite. This encouraging activity and selectivity led to the start of this series.

The synthesis of the cyclopenta[*c*]pyrazole nucleus begins with alkyne **4**, which is available in 4 steps from TMS-acetylene and ethyl 2-(oxiran-2-yl)acetate (Scheme 1).[8,9] Treatment of **4** with NBS and $AgNO_3$ gives the alkynyl bromide **5**.[10] Conversion to the hydrazide and then treatment with PS-PPh_3 and CCl_4 gives the hydrazonyl chloride **6**.[8] Subsequent generation of the nitrilimine and intramolecular 3+2 dipolar cycloaddition on the alkyne gives the cyclopenta[*c*]pyrazole **7**.[11] Installation of the 3-aryl substituent by Suzuki coupling and deprotection of the TIPS gives the key 5-hydroxycyclopenta[*c*]pyrazole **8**.[12]

A great deal of synthetic work was done functionalizing the 5-position of the cyclopenta[*c*]pyrazole ring system from the 5-hydroxy intermediate **8** (Scheme 2). Treatment with NaHMDS and MeI or *i*PrI gives the ether **9**; however, more substituted ethers were not accessible using this method. Treatment with NaHMDS and cyclohexanecarbonyl chloride gives the ester, which can be reduced with Et_3SiH in the presence of $InBr_3$ to give the ether **10**.[13] The cyclopentyl ether **11** was accessed by reacting with cyclopentene and PhSe-phthalimide in the presence of BF_3-OEt_2 to give the selenide intermediate, which was reduced with Bu_3SnH and AIBN.[14] The phenyl ether **12** was made by Mitsunobu reaction

* Corresponding author. Tel.: +1 215 628 7843; fax: +1 215 540 4611.
E-mail address: mwinter4@its.jnj.com (M.P. Winters).

http://dx.doi.org/10.1016/j.bmcl.2014.03.063
0960-894X/

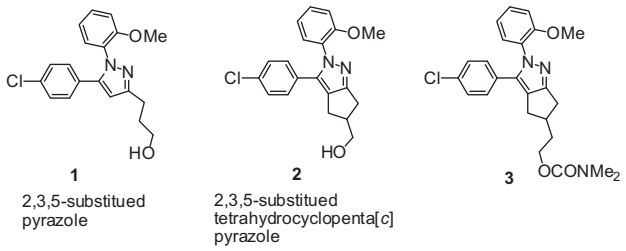

Figure 1. Initial pyrazole hit and proposed bicyclic pyrazoles.

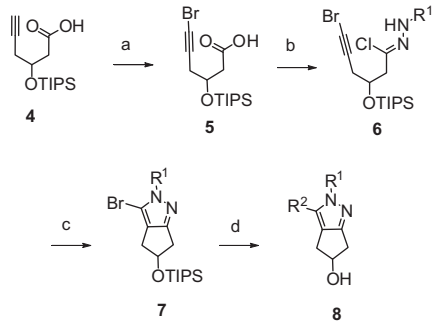

Scheme 1. Reagents and conditions: (a) NBS, $AgNO_3$; (b) (i) *i*-BuOCOCl, NMM, R^1NHNH_2, DCM, (ii) PS-Ph_3P, CCl_4, ACN, 50 °C; (c) TEA, toluene, 100 °C; (d) (i) $R^2B(OH)_2$, $Pd(OAc)_2$, (*o*-tol)$_3P$, Na_2CO_3, 80 °C, (ii) TBAF.

with phenol. Oxidation of the alcohol with Dess–Martin periodinane gives the ketone **13**, a versatile intermediate. Treatment with the appropriate diol and BF_3-OEt_2 gives the ketal **14**. The aryl and heteroaryl derivatives **15** were made from the ketone, by first making the vinyl triflate followed by Suzuki coupling and reduction of the double bond. Reductive amination of the ketone can give certain amine derivatives **16**.

Other amine derivatives at the 5-position were made by converting the alcohol to the amine and derivatizing from there (Scheme 3). Formation of the mesylate and displacement with azide gives **17**, which is hydrogenated to give amine **18**. Treatment

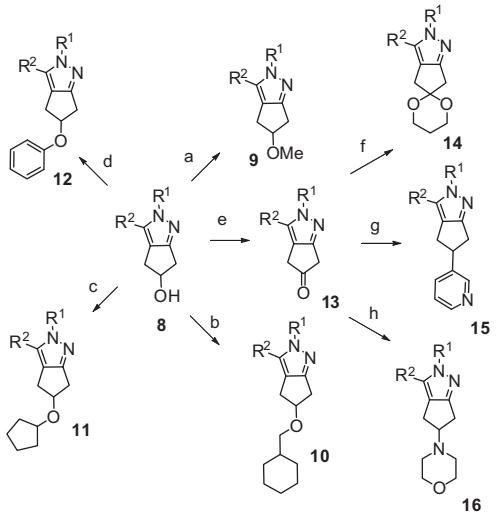

Scheme 2. Reagents and conditions: (a) NaH, MeI; (b) (i) NaHMDS, cyclohexanecarbonyl chloride, (ii) $InBr_3$, Et_3SiH; (c) (i) cyclopentene, PhSe-phthalimide, BF_3-OEt_2, (ii) Bu_3SnH, AIBN; (d) phenol, Ph_3P, DIAD; (e) Dess–Martin periodinane; (f) 1,3-propanediol, BF_3-OEt_2; (g) (i) KHMDS, $PhN(SO_2CF_3)_2$, (ii) 3-pyridyl pinacolboronate, $(Ph_3P)_4Pd$, (iii) H_2, PtO_2; (h) morpholine, $NaBH(OAc)_3$, HOAc.

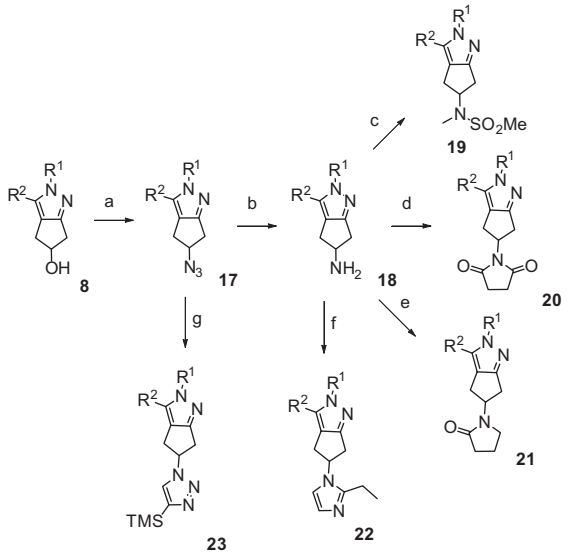

Scheme 3. Reagents and conditions: (a) (i) TEA, MsCl, (ii) NaN_3, DMF, 100 °C; (b) H_2, 10% Pd/C; (c) (i) TEA, MsCl, (ii) NaHMDS, MeI; (d) succinimide, TEA, toluene, 110 °C; (e) (i) 4-chlorobutanoyl chloride, K_2CO_3, (ii) NaHMDS; (f) propionaldehyde, glyoxal, NH_4OAc; (g) TMS-acetylene, CuI, DIEA.

of **17** with a sulfonyl chloride gives the sulfonamide, which can be alkylated on nitrogen giving **19**. Reaction with succinic anhydride gives the succinimide **20**, whereas condensation with 4-chlorobutanoyl chloride gives the lactam **21**. Imidazoles **22** can be made by reaction with aldehydes in the presence of glyoxal and ammonia. Click chemistry on the intermediate azide **17** gives the triazole **23**.

From the straight-chain pyrazole hits from the HTS campaign, *ortho*-substitution on the aryl ring at the 2-position of the pyrazole was critical for activity, and the *o*-methoxy **1** was particularly potent (Table 1). Removal of the methoxy **24**, or moving the methoxy to the *m*- or *p*-positions **25** and **26** lost potency, as did the 2-CF_3 **27**, 2-OH **28** and 2-O*i*Pr **29**. 4-Chloro was one of the best substituents on the phenyl ring at the 3-position of the pyrazole; removal resulted in a loss of potency **30**. The acid functionality on the side-chain abolished activity **31**. This SAR led us to attempt to enhance the potency by making dramatic changes at the 5-position of the cyclopentylpyrazole wherein many different substituents were tolerated. It was hoped that these changes would also

Table 1
SAR of pyrazoles from HTS campaign

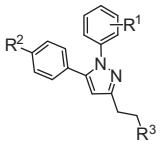

Compd No.	R^1	R^2	R^3	FDSS IC_{50} (nm)
1	2-OMe	Cl	CH_2OH	100
24	H	Cl	CH_2OH	1200
25	3-OMe	Cl	CH_2OH	690
26	4-OMe	F	CH_2OH	2370
27	2-CF_3	Cl	CH_2OH	790
28	2-OH	Cl	CH_2OH	2300
29	2-O*i*Pr	Cl	CH_2OH	260
30	2-OMe	H	CH_2OH	16%[b]
31	2-OMe	Cl	COOH	29%[a]

[a] % Inhibition at 5 μM.
[b] % Inhibition at 1 μM.

Table 2
SAR of 5-ethers and 5-heterocycles

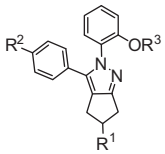

Compd No.	R^1	R^2	R^3	FDSS IC_{50} (nm)	RLM[a] (%)
32	OMe	Cl	Me	52	2
33	O*i*Pr	Cl	Me	5.7	3
34	*O*-Cyclopentyl	Cl	Me	22	19
35	OPh	Cl	Me	130	54
36	OCH_2-cyclohexyl	Cl	Me	130	25
37	Pyrid-3-yl	Cl	Me	8.6	14
38	4-Cyclopropylpyrid-3-yl	Cl	Me	280	98
39	Imidazole	Cl	Et	38	86
40	4,5-Di-Et-imidazole	CN	Me	37	2
41	2-Et-imidazole	CN	Me	200	21
42	Morpholine	Cl	Me	16	1
43	Pyrrolidone	Cl	Et	19	3
44	Triazole	Cl	Me	19	8
45	Succinimide	Cl	Et	7.5	2

[a] % Remaining after 10 min incubation with rat liver microsomes.

enhance the RLM stability because the HTS hits and the initial SAR on a very similar series, the 2,3,5-tetrahydropyrrolo[3,4-*c*]pyrazoles (N in the ring at the 5-position of the bicycle), indicated it would be difficult to replace the *o*-methoxy and maintain potency.[15]

One series of compounds evaluated were ethers and heteroaryls at the 5-position (Table 2). Methyl ether **32** was modestly potent against N-type in the FDSS assay, and adding some bulk gave the most potent compound in this series, the isopropyl **33**.[7] Increasing the size further gave less potent compounds, such as cyclopentyl **34**. Phenyl **35** was particularly poor as were the compounds with methylene spacers, such as **36**. Potency and RLM stability in this series appear to be inversely correlated. We attempted to improve solubility in the 5-heteroaryl series by making pyridyl **37**; however, this compound suffered from poor metabolic stability. Increasing bulk at the 4-position of the pyridyl **38** decreased the potency. One attempt to increase solubility, N-linked imidazole **39**, had moderate potency and excellent RLM stability (86% remaining after 10 min incubation with RLM). It also was much more soluble in aqueous media than previous compounds. Attempts to build the potency back by adding alkyl groups to the imidazole were unsuccessful, as shown by **40** and **41**. Other N-heterocyles, such as morpholine **42**, pyrrolidone **43**, triazole **44** and succinimide **45**, were more potent but lacked RLM stability.

Two series of compounds that were initially promising were the 5-spirocyclic ketals and the sulfonamides (Table 3). Unsubstituted propyl ketal **46** was 50 nM. Adding bulk to the ketal ring by making the 2,2-dimethylpropyl ketal **47** and pinacol ketal **48** improved potency. An attempt to increase solubility by replacing the 4-chlorophenyl with 4-dimethylaminophenyl **49** maintained potency but reduced RLM stability. Introduction of pyridyl at R^3 **50** lowered the potency but maintained stability. In the sulfonamide series, excellent potency was achieved by sulfamide **51** and sulfonamide **52**, whereas demethylation of these functional groups resulted in a loss in potency. Attempts to increase the aqueous solubility of the series by introducing a pyridyl at R^3 **54** lowered the potency. Most of the sulfamides and sulfonamides lacked appreciable RLM stability.

A set of some of the more active compounds were tested in secondary patch clamp assays[16] and a more physiologically relevant ex vivo calcitonin gene-related peptide (CGRP) release assay[17] using rat spinal cord slices (Table 4). In general, there was good correlation between the FDSS assay and the QPatch assay. It has been postulated that relatively greater inhibition at high versus low frequency may result in an improved therapeutic index, and many of the compounds exhibited this characteristic.[18] Of the compounds tested in the CGRP release assay, compound **47** stands out as being more active than predicted by its FDSS and QPatch potencies.

Following the secondary assays, compounds **47**, **48** and **51** were evaluated in the rat Complete Freund's Adjuvant (CFA) radiant heat model of inflammatory pain due to their potency and relative stability.[19] Only ketal **47** at 30 mpk PO showed effects in lengthening paw withdrawal latencies while the others had no effect (Fig. 2).[20] An IV only pharmacokinetic study in rats showed that after a 0.4 mg/kg dose of **47**, the initial concentration c_0 was 199 ng/mL, the AUC_{last} was 98 h ng/mL, the volume of distribution at steady state was 4.8 L/kg indicating extensive tissue distribution, clearance was high at 62.7 mL/min/kg, and the $t_{1/2}$ was 1.3 h. A tissue distribution study in rats 1 h after an oral dose of 30 mg/kg **47** showed 133 ng/g in brain (tissue/plasma ratio 3.95), 109 ng/g in spinal cord (tissue/plasma ratio 3.24), and below levels of

Table 3
SAR of 5-ketals and 5-sulfonamides

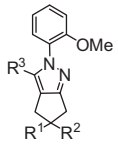

Compd No.	R^1	R^2	R^3	FDSS IC_{50} (nm)	RLM[a] (%)
46	$-O(CH_2)_3O-$		4-Cl-Ph	50	21
47	$-OCH_2C(Me)_2CH_2O-$		4-Cl-Ph	22	18
48	$-OC(Me)_2C(Me)_2O-$		4-Cl-Ph	6.6	2
49	$-OC(Me)_2C(Me)_2O-$		4-Me_2N-Ph	3.0	4
50	$-OC(Me)_2C(Me)_2O-$		4-Me-pyrid-3-yl	19	18
51	$NMeSO_2NMe_2$	H	4-Cl-Ph	3.1	6
52	$NMeSO_2Me$	H	4-Cl-Ph	6.4	8
53	$NHSO_2NMe_2$	H	4-Cl-Ph	14	2
54	$NHSO_2Me$	H	4-Cl-Ph	26	18
55	$NMeSO_2NMe_2$	H	4-MeO-pyrid-3-yl	13	1

[a] % Remaining after 10 min incubation with rat liver microsomes.

Table 4
Patch clamp and CGRP release data for selected compounds

Compd No.	FDSS IC_{50} (nm)	QPatch Lo freq[a]	QPatch Hi freq[a]	QPatch ratio Lo/Hi (%)	CGRP release[b]	RLM[c] (%)
39	38	13	29	45	21	86
48	6.6	37	48	77	77	21
47	22	21	37	57	63	18
51	3.1	37	59	63	54	6
52	6.4	44	46	96	NT	8
33	5.7	48	61	79	NT	3
45	7.5	47	53	89	NT	2
42	16	33	31	106	NT	1

[a] % Inhibition at 0.1 μM.
[b] % Inhibition at 1.0 μM.
[c] % Remaining after 10 min incubation with rat liver microsomes.

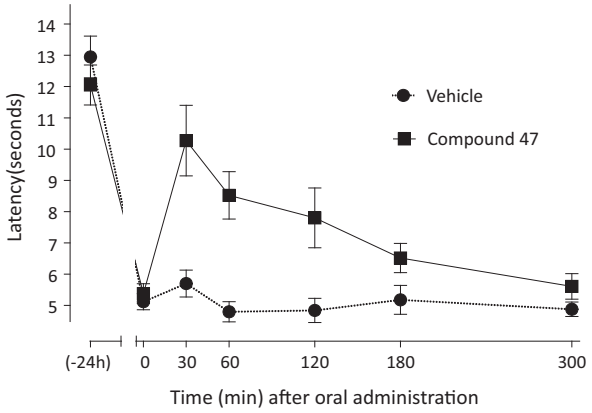

Figure 2. Compound **47** in the rat CFA model of pain.

quantitation in both brain and spinal cord extracellular fluid. These studies show that reasonable concentrations of **47** can be achieved in the target tissues brain and spinal cord.

In summary, we developed a novel scaffold with improved potency for N-type calcium channel from a very simple pyrazole hit. Although identifying a compound in this series with relatively high N-type potency and RLM stability was a challenge, ketal **47** nonetheless demonstrated robust efficacy in the rat CFA model of inflammatory pain and showed efficacious concentrations could be achieved in brain and spinal cord. While much work remains, this novel series of N-type calcium channel inhibitors may lead to candidates for analgesic drugs with improved therapeutic index in the future.

Acknowledgments

The authors gratefully acknowledge the ADME and analytical teams in Spring House for running the RLM assays and the PK and tissue distribution studies, and Renee DesJarlais for initial modeling discussions.

References and notes

1. (a) Schroeder, C.; Doering, C.; Zamponi, G.; Lewis, R. *Med. Chem.* **2006**, *2*, 535; (b) Elmslie, K. *J. Neurosci. Res.* **2004**, *75*, 733; (c) Belardetti, F. *Future Med. Chem.* **2010**, *2*, 791; (d) Lee, S. *Curr. Neuropharmacol.* **2013**, *11*, 606.
2. McGivern, J. In Peripheral Receptor Targets for Analgesia: Novel Approaches to Pain Management; Cairns, B., Ed.; John Wiley & Sons, Hoboken, NJ 2009, pp. 111–135.
3. McGivern, J.; McDonough, S. *Curr. Drug Targets CNS Neurol. Disord.* **2004**, *3*, 457.
4. (a) Prommer, E. *Drugs Today* **2006**, *42*, 369; (b) Miljanich, G. *Curr. Med. Chem.* **2004**, *11*, 3029.
5. (a) Yamamoto, T.; Ohno, S.; Niwa, S.; Tokumasu, M.; Hagihara, M.; Koganei, H.; Fujita, S.; Takeda, T.; Saitou, Y.; Iwayama, S.; Takahara, A.; Iwata, S.; Shoji, M. *Bioorg. Med. Chem. Lett.* **2011**, *21*, 3317; (b) Tyagarajan, S.; Chakravarty, P.; Park, M.; Zhou, B.; Herrington, J.; Ratliff, K.; Bugianesi, R.; Williams, B.; Haedo, R.; Swensen, A.; Warren, V.; Smith, M.; Garcia, M.; Kaczorowski, G.; McManus, O.; Lyons, K.; Li, X.; Madeira, M.; Karanam, B.; Green, M.; Forrest, M.; Abbadie, C.; McGowan, E.; Mistry, S.; Jochnowitz, N.; Duffy, J. *Bioorg. Med. Chem. Lett.* **2011**, *21*, 869; (c) Yamamoto, T.; Takahara, A. *Curr. Top. Med. Chem.* **2009**, *9*, 377; (d) Pajouhesh, H.; Feng, Z.; Zhang, L.; Pajouhesh, H.; Jiang, X.; Hendricson, A.; Dong, H.; Tringham, E.; Ding, Y.; Vanderah, T.; Porreca, F.; Belardetti, F.; Zamponi, G.; Mitscher, L.; Snutch, T. *Bioorg. Med. Chem. Lett.* **2012**, *22*, 4153; (e) Beebe, X.; Yeung, C.; Darczak, D.; Shekhar, S.; Vortherms, T.; Miller, L.; Milicic, I.; Swensen, A.; Zhu, C.; Banfor, P.; Wetter, J.; Marsh, K.; Jarvis, M.; Scott, V.; Schrimpf, M.; Lee, C.-H. *Bioorg. Med. Chem. Lett.* **2013**, *23*, 4857.
6. Only certain compounds were intermittently assayed for selectivity versus L-type Calcium Channel during this program. No further L-type selectivity data is available.
7. (a) Finley, M.; Lubin, M.; Neeper, M.; Beck, E.; Liu, Y.; Flores, C.; Qin, N. *Assay Drug Dev. Technol.* **2010**, *8*, 685
(a) In the FDSS assay, functional activity of test compounds are determined by their inhibitory effects on Ca^{2+} influx via N-type calcium channel after depolarizing plasma membrane with 50 mM KCl. Calcium mobilization responses to KCl depolarization are evaluated by measuring the intensity of Ca^{2+} fluorescent signal in the presence of BD Calcium Assay Dye (BD Biosciences), utilizing a Functional Drug Screening System (FDSS) by Hamamatsu. The percent inhibition at a concentration of 1 μM as well as IC_{50} values will be reported. For this screen, a stable cell line (HEK parent) expressing Cav2.2 (N-type calcium channel, Genbank accession number AAO53230) subunits is used. Cav2.2 subunits were expressed in pcDNA3.1 and pBudCE4.1 vectors under selection by 400 μg/ml of G418 and 200 μg/ml of Zeocin. Cells were clonally isolated, expanded and screened by Western blot analyses, and further tested for expression of characteristic N-type calcium currents by whole-cell patch clamp. HEK293 cells stably expressing Cav2.2 subunits are routinely grown as monolayer in Dulbecco's Modification of Eagle's Medium (DMEM; low glucose Cat # 12320-032) supplemented with 10% FBS, 2 mM L-glutamine, 100 I.U./ml penicillin, 100 μg/ml streptomycin, 400 μg/ml G418, and 200 μg/ml Zeocin (Split ratio: 1:5). Cells are maintained in 5% CO_2 at 37 °C. JNJ compounds are prepared as 10 mM stock in DMSO from neat, if available. Otherwise, the 5 or 10 mM DMSO stock solutions provided in-house are used. Calcium mobilization responses to KCl depolarization are evaluated by measuring the intensity of Ca^{2+} fluorescent signal in the presence of BD Calcium Assay Dye (BD Biosciences), utilizing a Functional Drug Screening System (FDSS) by Hamamatsu. 24 h prior to assay, cells are seeded in clear-base poly-D-lysine coated 384-well plates (BD Biosciences, NJ, USA) at a density of 5000 cells per well in culture medium and grown overnight in 5% CO_2 at 37 °C. On assay day, growth media is removed and cells are loaded with BD calcium assay dye (BD Bioscience) for 35 min at 37 °C, under 5% CO_2 and then for 25 min at room temp. Utilizing the FDSS, cells are challenged with test compounds (at varying concentrations) and intracellular Ca^{2+} is measured for 5 min prior to the addition of 50 mM KCl for an additional 3 min of measurement. IC_{50} values for compounds ran in this assay are determined from six-point dose–response studies and represent the concentration of compound required to inhibit 50% of the maximal response. Maximal fluorescence intensity (FI) achieved upon addition of 50 mM KCl was exported from the FDSS software and further analyzed using GraphPad Prism 3.02 (Graph Pad Software Inc., CA, U.S.A.). Data is normalized to the maximum average counts of quadruplicate wells for each data points in the presence of 50 mM KCl and to the minimum average counts in the presence of buffer. Theoretical curves are generated using nonlinear regression curve-fitting analysis of either sigmoidal dose response or sigmoidal dose response (variable slope) and the IC_{50} values with the best-fit dose curve determined by GraphPad Prism are reported. Conotoxin was run as a positive control in the assay and typically showed IC_{50}'s of 10–20 nM.
8. Winters, M.; Teleha, C.; Sui, Z. *Tetrahedron Lett.* **2014**, *55*, 2150.
9. Use of commercially available enantiomerically pure epoxide enables either enantiomer at the 5-position of the cyclopentylpyrazole to be made easily.
10. Leroy, J. *Synth. Comm.* **1992**, *22*, 567.
11. Padwa, A.; Nahm, S.; Sato, E. *J. Org. Chem.* **1978**, *43*, 1664.

12. The same compounds can be synthesized using an arylalkyne in place of the bromoalkyne if desired. See Ref. 8.
13. Sakai, N.; Moriya, T.; Konakahara, T. *J. Org. Chem.* **2007**, *72*, 5920.
14. Kim, K.; Choi, S.; Park, J.; Lee, Y.; Kim, J. *Tetrahedron: Asymmetry* **2001**, *12*, 2649.
15. Winters, M.; Subasinghe, N.; Wall, M.; Beck, E.; Brandt, M.; Finley, M.; Liu, Y.; Lubin, M.; Neeper, M.; Qin, N.; Flores, C.; Sui, Z. *Bioorg. Med. Chem. Lett.* **2014**, *24*, 2053.
16. Mathes, C.; Friis, S.; Finley, M.; Liu, Y. *Comb. Chem. High Thr. Screen.* **2009**, *12*, 78.
17. CGRP levels were evaluated using a Spi Bio rat CGRP enzyme linked immunoassay kit (Cayman Chemicals) as recommended by the manufacturer. By including samples with known amounts of CGRP in each enzyme immunoassay, a standard curve was created that permitted the conversion of absorbance to pg/mL CGRP for each of the unknowns, as determined using GraphPad Prism software. Percentage of inhibitions for the small-molecule evaluations were calculated using the following formula: % Inhibition = (Total Release − Test Sample)/(Total Release − Conotoxin) × 100 where Total Release = K^+-evoked (50 mM KCl) release, Test Sample = release in the presence of KCl plus test inhibitor, and Conotoxin = release in the presence of KCl plus 1 μM conotoxin (full block of Cav2.2), all in the presence of 1 μM nifedipine to block CGRP release due to L-type channel activity. Unless otherwise indicated, statistics for comparing among CGRP results utilized a one-way analysis of variance with Dunnett's test (Ref. 7a).
18. Winquist, R.; Pan, J.; Gribkoff, V. *Biochem. Pharmacol.* **2005**, *70*, 489.
19. Malmberg, A.; Gilbert, H.; McCabe, R.; Basbaum, A. *Pain* **2003**, *101*, 109. More detail on the CFA model.
20. Compound **39** was below the potency threshold to be tested in the CFA model. Perhaps the low RLM stability of **51** affected its in vivo activity. There is no explanation for the lack of activity of **48**; the compound has a very similar profile to **47**.